Satake *et al. Geosci. Lett. (2017) 4:33*
https://doi.org/10.1186/s40562-017-0099-y

Geoscience Letters

RESEARCH LETTER

Open Access

Different depths of near-trench slips of the 1896 Sanriku and 2011 Tohoku earthquakes

Kenji Satake[1*], Yushiro Fujii[2] and Shigeru Yamaki[3]

Abstract

The 1896 Sanriku earthquake was a typical 'tsunami earthquake' which caused large tsunami despite its weak ground shaking. It occurred along the Japan Trench in the northern tsunami source area of the 2011 Tohoku earthquake where a delayed tsunami generation has been proposed. Hence the relation between the 1896 and 2011 tsunami sources is an important scientific as well as societal issue. The tsunami heights along the northern and central Sanriku coasts from both earthquakes were similar, but the tsunami waveforms at regional distances in Japan were much larger in 2011. Computed tsunamis from the northeastern part of the 2011 tsunami source model roughly reproduced the 1896 tsunami heights on the Sanriku coast, but were much larger than the recorded tsunami waveforms. Both the Sanriku tsunami heights and the waveforms were reproduced by a 200-km × 50-km fault with an average slip of 8 m, with the large (20 m) slip on a 100-km × 25-km asperity. The moment magnitude M_w of this model is 8.1. During the 2011 Tohoku earthquake, slip on the 1896 asperity (at a depth of 3.5–7 km) was 3–14 m, while the shallower part (depth 0–3.5 km) slipped 20–36 m. Thus the large slips on the plate interface during the 1896 and 2011 earthquakes were complementary.

Keywords: Tsunami earthquake, Japan Trench, 1896 Sanriku earthquake, 2011 Tohoku earthquake

Background

The 11 March 2011 Tohoku earthquake (M_w 9.0) was the largest instrumentally recorded earthquake in Japan and caused devastating tsunami damage including ~ 18,500 casualties. The ground shaking was felt throughout the Japanese Islands with the maximum seismic intensity of 7 on the Japan Meteorological Agency (JMA) scale, or 11–12 on the Modified Mercalli scale (Fig. 1a). Huge slip (> 50 m) on the plate interface up to the Japan Trench axis was estimated near the epicenter (~ 38.5°N) from seismic waves (Ide et al. 2011), inland and submarine geodetic data (Iinuma et al. 2012), and tsunami waveforms (Fujii et al. 2011; Satake et al. 2013b). On the contrary, the largest tsunami heights on the Sanriku coast, ~ 40 m, were recorded ~ 100 km north (near 39.6°N). This enigma was explained by a delayed tsunami generation in the northern part of tsunami source through the tsunami waveform analysis (Satake et al. 2013b; Tappin et al. 2014). However, the cause of the delayed tsunami generation is still controversial, either due to slip on shallow plate interface (Satake et al. 2013b) or submarine landslide (Tappin et al. 2014).

In the northern part of the 2011 tsunami source, the 15 June 1896 Sanriku earthquake occurred and caused the worst tsunami disaster in Japan, with casualties of ~ 20, 000 (Shuto et al. 2007). The 1896 Sanriku earthquake was a typical example of a 'tsunami earthquake' (Kanamori 1972; Tanioka and Satake 1996b). The origin time: 19 h 32 m (local time), the epicenter: 144°E, 39.5°N, and magnitude: $M = 6.8$ were estimated from Japanese seismological data (Utsu 1979). The surface wave magnitude $M_S = 7.2$ was assigned from global data (Abe 1994). The moment magnitude M_w was estimated as 8.0–8.2, from a comparison of aftershock activity with other large earthquakes (Utsu 1994). The tsunami magnitude M_t was determined

*Correspondence: satake@eri.u-tokyo.ac.jp
[1] Earthquake Research Institute, The University of Tokyo, 1-1-1 Yayoi, Bunkyo-ku, Tokyo 113-0032, Japan
Full list of author information is available at the end of the article

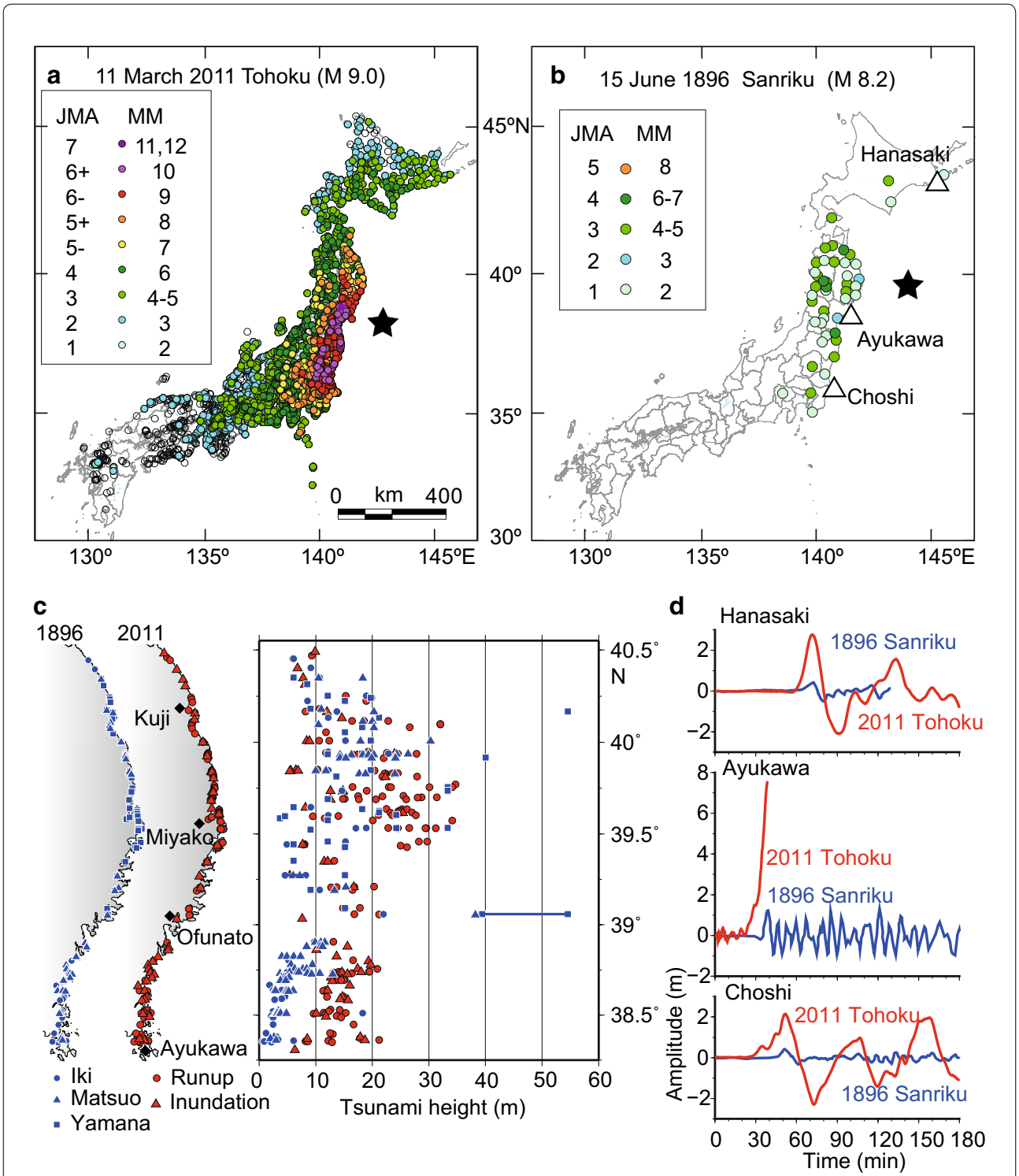

Fig. 1 **a** Epicenter (black star) and seismic intensity distribution of the 2011 Tohoku earthquake, according to Japan Meteorological Agency. **b** Epicenter and seismic intensity distribution of the 1896 Sanriku earthquake. Locations of tide gage stations (open triangles) are also shown. **c** Tsunami heights on the Sanriku coast from the 1896 Sanriku tsunami (blue symbols with different shapes for the data source) and the 2011 Tohoku earthquake (red symbols with different shapes for runup and inundation heights) from Tsuji et al. (2014). **d** Tsunami waveforms from the 1896 Sanriku (blue curves) and 2011 Tohoku (red curves) earthquakes recorded at the three tide gage stations

as 8.6 from global data (Abe 1979) and 8.2 from Japanese data (Abe 1981). The ground shaking was weak (2–3 on the JMA seismic intensity scale, corresponding to 4–5 on the Modified Mercalli scale; Fig. 1b). However, the tsunami heights on the Sanriku coast from the 2011 and 1896 earthquakes were roughly similar (Fig. 1c, Tsuji et al. 2014) as detailed in the "Tsunami data of the 1896 earthquake."

Tsunami waveform modeling of the 1896 Sanriku earthquake has shown that slip occurred on a narrow fault located near the trench axis (Tanioka and Satake 1996b; Tanioka and Seno 2001). This is a common feature of 'tsunami earthquakes' such as the 1992 Nicaragua or 2010 Mentawai earthquakes (Satake and Tanioka 1999; Satake et al. 2013a). Tanioka et al. (1997) further proposed that the 1896 Sanriku 'tsunami earthquake' occurred in a region where the ocean bottom topography is rough, characterized by well-developed horst and graben structures. Polet and Kanamori (2000) extended this model to global subduction zones, based on the examination of the source spectra of large ($M > 7$) earthquakes in the 1990s. More recently, Lay et al. (2012) classified the seismogenic zone of subduction zones into four domains and assigned the shallowest domain (A: less than 15 km depth) as a source region of 'tsunami earthquakes.'

After the occurrence of the 2011 Tohoku earthquake and tsunami, a question arose about the relation between the 1896 and 2011 tsunami sources. Did both earthquakes rupture the same shallow plate interface or different parts? Why was the 1896 event a 'tsunami earthquake' while the 2011 earthquake was not? These are important issues both in science of tsunami generation in subduction zones, particularly near the trench axis, and also for tsunami hazard assessment.

In this study, we re-estimate the slip distribution, particularly in depth direction, of the 1896 Sanriku 'tsunami earthquake' based on both tsunami heights on the Sanriku coast and the tsunami waveforms recorded on three tide gage stations at regional distance in Japan. It should be noted that tsunami height data on the Sanriku coast have not been used in the previous studies of the 1896 earthquake. In order to find the best 1896 tsunami source model, we start from the northern part of the 2011 source model, compute the tsunami heights on the Sanriku coast and tsunami waveforms at tide gage stations, and compare them with the 1896 observations. We also compare the tsunami source models, or obtained slip distributions, of the 1896 and 2011 earthquakes, and discuss why the 2011 earthquake was not a 'tsunami earthquake.'

Tsunami data of the 1896 earthquake

The 1896 tsunami was instrumentally recorded on three tide gage stations at regional distances in Japan: Hanasaki (440 km from the epicenter), Ayukawa (250 km), and Choshi (500 km) (Fig. 1b, Honda et al. 1908; Imamura and Moriya 1939). Tanioka and Satake (1996b) examined these waveforms, estimated the clock timing errors as large as 5 min, and modeled the waveforms without timing information. The 2011 tsunami was also recorded at these tide gage stations, although the Ayukawa record went off-scale immediately following the first tsunami arrival at ~ 30 min from the earthquake (Satake et al. 2013b). Comparison of the 1896 and 2011 tsunami waveforms indicates that both periods and amplitudes of the 2011 waveforms are larger than those of the 1896 tsunami (Fig. 1d), probably due to the different sizes of tsunami source.

For the 1896 tsunami heights along the Sanriku coasts, at distances ranging from 170 to 250 km from the epicenter, field surveys were made by three groups (Fig. 1c). Yamana (reproduced by Unohana and Ota 1988) made a post-tsunami survey from July through September of 1896 in all of the 37 villages along the Sanriku coast. The largest heights of 55 m were reported at two locations. While his report contains 168 diagrams, the reliability of his measurements has been questioned (Shuto et al. 2007). Iki (1897) made a survey in June and July of 1896 along the Sanriku coast. He measured tsunami heights based on various kinds of traces and eyewitness accounts, and assigned different reliabilities depending on the kind of data. The maximum tsunami height was 24 m at Yoshihama. In 1933, another devastating tsunami, with maximum height of 29 m and approximately 3000 fatalities, was caused by the 1933 Sanriku earthquake (M_s 8.5). Matsuo (1933) made field survey to measure the heights of both 1896 and 1933 tsunamis. Although the 1896 tsunami heights were measured 37 years after the occurrence based on the eyewitness accounts, the survey points were plotted on 1:50,000 maps and provided valuable information. The often-quoted maximum height of 38 m at Shirahama from the 1896 Sanriku tsunami was based on his report. In this study, we adopt the reported tsunami heights by Iki (1897) and Matsuo (1933) and compare them with the calculated heights. Because of the sawtooth-shaped topography of the Sanriku coast, often called a ria-type coast in Japan, both the 1896 and 2011 tsunami heights significantly change at short distance (Fig. 1c). Tsuji et al. (2014) compared the 1896 and 2011 tsunami heights on the Sanriku coast and found the median ratios (1896/2011) are 1.01, 0.85, and 0.29 on the northern, central, and southern Sanriku coasts, respectively, and 0.69 for the entire Sanriku coast. These indicate that the 1896 tsunami heights were similar to the 2011 tsunami heights on the northern and central Sanriku coasts.

A careful manual observation of the tsunami was conducted at the Miyako meteorological observatory

(Miyako is shown in Fig. 1c), and published in the annual report of the Central Meteorological Observatory (1902). It describes as follows. "At 19 h 32 m 30 s (local time), a weak shock of earthquake was felt, lasting for about 5 min. Its direction was ENE–WSW and the nature was extremely slow. At about 19 h 50 m, the sea began to recede. At about 20 h, the water rose, but fell somewhat in a few minutes. At 20 h 07 m, the biggest wave of about 4.5 m high came in with a fearful booming sound, and instantly swept away all houses or living things that were in its path. Subsequently, six waves of more or less heights came until the noon of the following day." At the Miyako observatory, seismograph observation already started in those days (Omori and Hirata 1899), hence the observer must be sensitive to accurate timing. In addition, the tsunami arrival times were measured relative to the earthquake. Therefore the timing of tsunami arrival at Miyako provides additional important information.

Tsunami computations

We use the subfault configuration of the 2011 Tohoku earthquake of Satake et al. (2013b). Only eight subfaults (0A to 1D: Fig. 2a, Table 1) in the northern and shallow part of the source are adopted. Each subfault is 50 km long and 25 km wide. The strike, dip, and slip angles are 193°, 8°, and 81°, respectively. The subfaults are placed on the Pacific plate (Nakajima and Hasegawa 2006), and the top depths beneath seafloor are 0 and 3.5 km for shallowest (row 0) and next (row 1) subfaults (Table 1). Seafloor

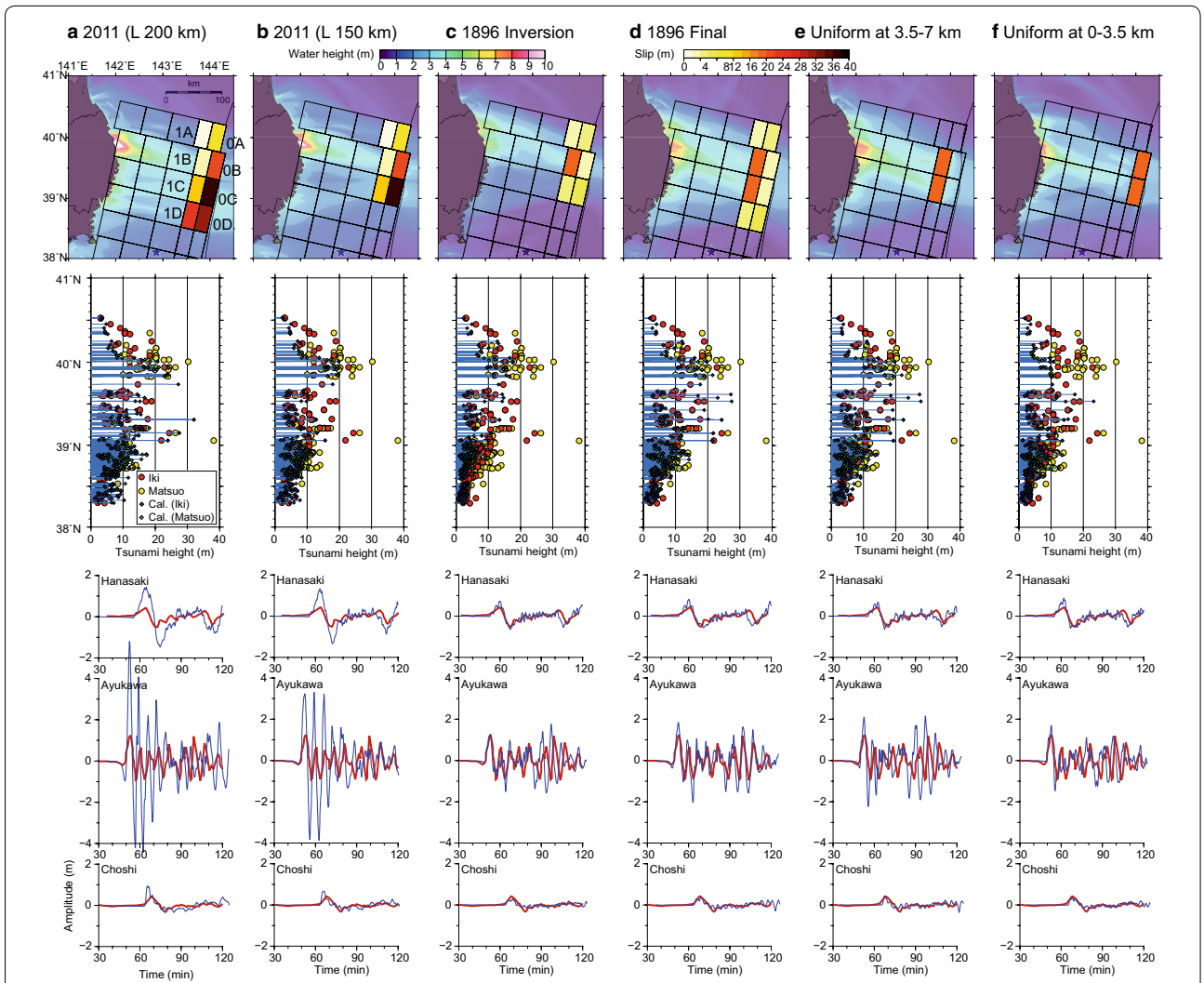

Fig. 2 Comparison of 6 models **a** 2011 model with 8 subfaults and 200 km long, **b** 2011 model with 6 subfaults and 150 km long, **c** 1896 inversion model, **d** 1896 final model, **e** uniform (20 m) slip at 3.5–7 km depth, **f** uniform (20 m) slip at 0–3.5 km depth. (top) Slip distribution on subfaults (color bar scale in the right) and computed maximum tsunami height (color bar scale in the left) for 6 models. (middle) Observed and computed tsunami heights on the Sanriku coast. Red and yellow circles show observed heights by Iki (1897) and Matsuo (1933), respectively. Blue and green circles with bars are computed heights on 6″ grid. (bottom) Tsunami waveforms at three tide gage stations at regional distances. Red curves are observed waveforms and blue curves are computed ones

Table 1 Subfault locations and the slip amounts for four source models

No.	Lat.(°N)*	Lon.(°E)*	2011 8 subfaults (m)	2011 6 subfaults (m)	1896 inversion (m)	1896 final (m)	Sum 1896 + 2011 (m)	Ratio 2011/1896
0A	40.198	144.35	11	11	6	6	16	1.9
1A	40.24809	144.06599	1	1	3	3	4	0.3
0B	39.738	144.331	21	21	3	3	23	7.6
1B	39.78808	144.04,888	3	3	20	20	23	0.2
0C	39.3	144.2	36	36	7	3	39	13.4
1C	39.35008	143.91966	14	14	5	20	33	0.7
0D	38.862	144.069	31	0	0	7	37	4.5
1D	38.91208	143.7904	22	0	0	5	28	4.4

* Location (latitude [Lat.] and longitude [Lon.]) indicates the northeast corner of each subfault. The fault length: 50 km, the fault width: 25 km, the strike: 193°, the dip angle: 8°, and the slip angle: 81° are common to all the subfaults. The top depths are 0 km and 3.5 km beneath seafloor, for subfaults 0* and 1*, respectively

displacement is calculated for a rectangular fault model in an elastic half-space (Okada, 1985). We also consider the effects of horizontal displacement on a steep bathymetric slope (Tanioka and Satake 1996a).

The non-linear shallow-water equations including advection and bottom friction terms and the equation of continuity on the spherical coordinate system are numerically solved (Satake 1995). We adopt the finite-difference method with the grid interval of 6″ (140 to 190 m). The bathymetry data are sampled from J-EGG500 (mesh data with 500 m interval provided by Japan Oceanographic Data Center) and M-7000 series digital bathymetry chart (provided by Japan Hydrographic Association), but newer coastal topography such as breakwater around tide gage stations are removed to reproduce the situation in 1896. The tide gage station at Choshi was located at 35° 44.0′N, 140° 50.4′E, different from the current location. The computations are made for 3 h after the origin time with a time step of 0.3 s.

For the Sanriku coast, additional computations including inundation on land with the finest grid size of 75 m are also made, and the computed tsunami heights are compared with the 143 heights reported by Iki (1897) and the 260 heights reported by Matsuo (1933) (Fig. 3, Additional file 1: Table S1, Additional file 2: Table S2). To quantify the comparison, the geometric mean K and geometric standard deviation κ of observed and computed heights (Aida 1978) are computed. If K is larger than one, the observed heights are larger than the computed ones. The geometric standard deviation can be considered as an error factor. The smaller κ means the smaller scatter hence the better model.

The 1896 tsunami source models

We first adopt the northeastern eight subfaults of the 2011 Tohoku earthquake tsunami source model (Satake et al. 2013b). The slips on the shallowest subfaults along the axis (row 0, depth of 0–3.5 km) are 11–36 m, whereas those on row 1 at the depth of 3.5–7 km range from 1 to 22 m. The average slip for the eight subfaults is 17 m, yielding the seismic moment of 3.5×10^{21} Nm and the corresponding moment magnitude M_w of 8.3, assuming the rigidity of 2×10^{10} N/m^2. The computed tsunami heights are similar to the observed heights on the northern Sanriku coast, but larger than those on the southern coast (Figs. 2a, 3). The geometric mean K is 0.70 and the geometric standard deviation κ is 1.56 for a total of 403 tsunami heights reported by Iki (1897) and Matsuo (1933) (Additional file 1: Table S1, Additional file 2: Table S2).

Because the eight subfaults of the 2011 model produced larger tsunami heights than the observed values on the southern Sanriku coast, we drop the southernmost subfaults (0D and 1D), and adopt the six subfaults. The average slip becomes 14 m, the seismic moment is 2.1×10^{21} Nm, and $M_w = 8.2$. The computed tsunami heights on the southern Sanriku coast become smaller and similar to the observed (Figs. 2b, 3). The geometric mean K becomes 0.93, indicating that observed and computed heights are almost the same, and the geometric standard deviation κ is 1.50. However, the computed tsunami waveforms at regional distances are much larger than the recorded ones, particularly at Hanasaki and Ayukawa (Fig. 2b). Thus the slip distribution of the 2011 Tohoku tsunami model, either six or eight subfaults, can reproduce the tsunami heights on the Sanriku coast but overestimates the tsunami waveforms at the tide gage stations located at regional distances. This is expected from the comparison of the 1896 and 2011 data; the tsunami heights are similar on the Sanriku coast, but the amplitude and period of tsunami waveforms are very different (Fig. 1c, d).

In order to find a model that explains the tsunami waveforms, we conduct inversion of the 1896 tsunami

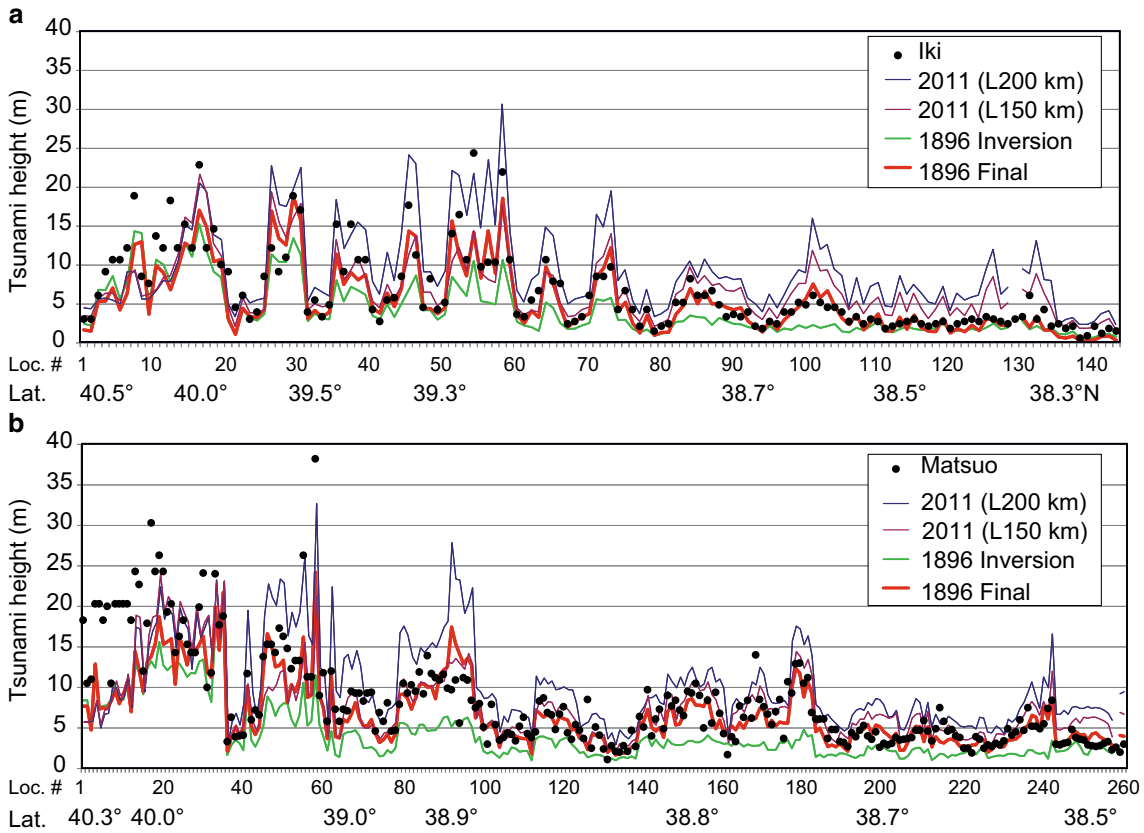

Fig. 3 Tsunami heights on the Sanriku coast reported by (**a**) Iki (1897) and (**b**) Matsuo (1933) are shown by black circles. Computed tsunami heights on 75 m grids for the four different models are shown by colored lines. Note that the scale for horizontal axis is location numbers (Additional file 1: Table S1, Additional file 2: Table S2), not distance. The latitudes for the locations are also shown

waveforms recorded at three tide gage stations. Because of poor timing accuracy, the observed waveforms are shifted so that the initial motion of observed and computed waves is aligned. The inversion method is similar to Satake et al. (2013b), but only the spatial slip distribution is estimated. The inversion model (Fig. 2c) shows large (20 m) slip on subfault 1B, deeper and second northernmost subfault. The slip on other five subfaults ranges 3–7 m, and the average slip is 7 m, which yields seismic moment of 1.1×10^{21} Nm and the moment magnitude of $M_w = 8.0$. This model is basically similar to that of Tanioka and Satake (1996b), although their average slip is smaller (5.7 m) and the dip angle is larger (20°). The tsunami heights on the Sanriku coast computed from this model are smaller than the observations (Figs. 2c, 3). The geometric mean K is 1.87, and the geometric standard deviation κ is 1.46. This model reproduces tsunami waveforms at regional distances but underestimates the Sanriku tsunami heights, particularly on the southern Sanriku coast.

We finally extend the large (20 m) slip to the southern subfault (1C) (Fig. 2d). The average slip on the eight subfaults is 8 m, yielding the seismic moment of 1.6×10^{21} Nm and the moment magnitude of $M_w = 8.1$. The computed tsunami heights on the Sanriku coast become larger, particularly on the southern Sanriku coast, and the geometric mean K becomes 1.11 with the geometric standard deviation of $\kappa = 1.39$ (Fig. 3, Additional file 1: Tables S1, Additional file 2: Table S2). The computed tsunami waveform at Ayukawa, located at the southern Sanriku coast, also becomes larger than the previous model. However, the computed tsunami waveforms at regional distances (Hanasaki and Choshi) are very similar to the previous model and the observed ones. This model explains both tsunami heights on the Sanriku coast and the recorded tsunami waveforms, and yields the smallest κ, hence considered as the best model of the 1896 Sanriku earthquake.

As mentioned in "Tsunami data of the 1896 earthquake," there is an additional observation of the 1896 Sanriku tsunami: tsunami arrival times at Miyako observatory. They reported that sea water started to recede at 18 min, and the maximum tsunami of 4.5 m was observed

at 35 min after the earthquake. To compare with these reports, we compute the tsunami waveforms at Miyako (Fig. 4). The tsunami waveform from the 1896 final model shows initial negative wave followed by the positive wave with an amplitude of ~ 3.4 m at around 35 min. While this is slightly smaller than the observed value, the timing is similar to the reported. The timing of the peak amplitude from the 2011 model is later (Fig. 4).

Effect of fault depth on tsunami heights

The final model of the 1896 Sanriku earthquake consists of large (20 m) slip with smaller (3–7 m) slips around it. In order to examine the effects of the small slips around the largest one, we trim these smaller slips and compute tsunamis from a uniform 20 m slip model on a 100-km × 25-km fault at a depth of 3.5–7 km (Fig. 2e). The tsunami heights on the Sanriku coast are similar to the above final model ($K = 1.32$), while the computed tsunami waveforms are slightly different; the periods of the first wave become shorter and the amplitude at Ayukawa is slightly larger.

For comparison, we also test another model of uniform 20 m slip, with the same size, at shallowest (0–3.5 km) part (Fig. 2f). The tsunami heights on the Sanriku coast from this model are smaller ($K = 1.63$), while the tsunami waveforms at regional distances are similar to those from the previous uniform-slip model at 3.5–7 km depth.

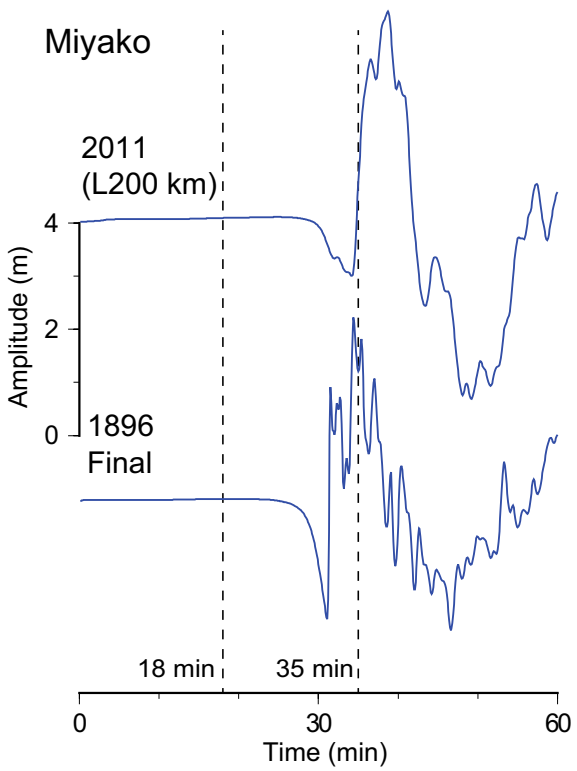

Fig. 4 Tsunami waveforms computed at Miyako from the 2011 model (8 subfaults) and the 1896 final model. Dashed lines (18 min and 35 min after the earthquake origin time) indicate the observed tsunami arrivals of first and maximum waves (see text)

These models indicate that the tsunami heights on the Sanriku coast are larger from slip on the deeper subfaults (3.5–7 km depth) than that on the shallowest subfaults (0–3.5 km depth). Two factors may contribute to this difference: distance from the source to the coast and the seafloor displacement due to faulting at different depths. The deeper subfaults are located closer to the coast than shallowest subfaults, thus the tsunami heights are larger on the coast. In addition, the deeper (3.5–7 km) subfaults produce larger seafloor displacements than surface rupture (top depth of 0 km), hence the tsunami heights are also larger. The water depth at these subfaults are also different: the water is deeper for the shallower subfaults near the trench axis. However, additional tests indicate that the water depth difference makes an insignificant effect for the tsunami heights on the Sanriku coast.

Comparison of 1896 and 2011 sources

During the 1896 Sanriku earthquake, the large (20 m) slip occurred on subfaults (1B and 1C: Table 1) at a depth of 3.5–7 km. The slips on surrounding subfaults range 3–7 m, including the shallowest subfaults (0–3.5 km). During the 2011 Tohoku earthquake, large slips (> 10 m) occurred at the shallowest subfaults. On the subfaults where the 1896 slip was large (1B and 1C), the 2011 slips were 3 and 14 m (Fig. 5). The slip ratio (2011/1896) is smaller than one in the deeper (3.5–7 km) subfaults except for the southern one (1D), while the ratio ranges 1.9–13 on the shallowest subfaults (Table 1).

This indicates that the 2011 northern slip near the trench axis, delayed ~ 3 min of the main slip near the epicenter, occurred on parts where the 1896 slip was not very large. The sum of subfault slip ranges from 20 to 40 m on shallowest subfaults (rows 0). The plate convergence rate is about 8 m per century (e.g., Sella G et al. 2002), hence these may correspond to 250–500 years of slip deficit.

Although the depths of largest slip of the 1896 and 2011 earthquakes were different, the frictional properties on these shallowest subfaults may be similar. Takahashi et al. (2004) estimated the seismic velocity structure along the northern Japan Trench by using the wide-angle airgun and ocean bottom seismogram data. The closest profile to the 1896 Sanriku earthquake source (Fig. 6) indicates that both faults are located at the contact zone between deformed area ($Vp = 3.2$–2.6 km/s) and oceanic crust ($Vp = 5.3$–5.6 km/s), suggesting similarities of fault zone properties. Hence the complimentary slips of the 1896 and 2011 earthquakes indicate slip partitioning of these events.

If the 2011 northern slip occurred at shallower part than the 1896 source, a question might arise why the

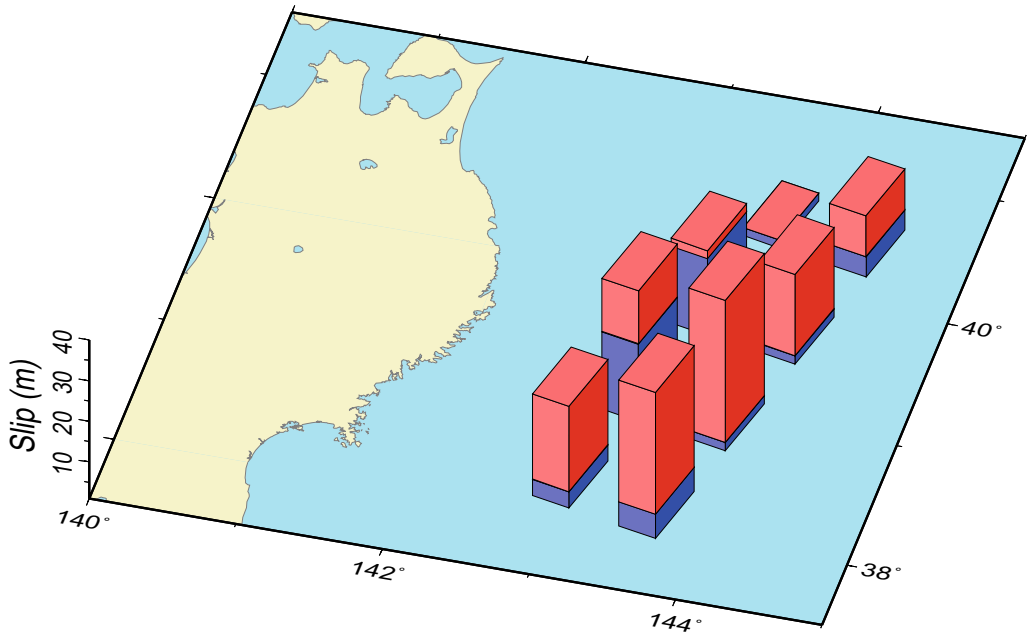

Fig. 5 Cumulative slips on subfaults of the 2011 (red columns) and 1896 (blue) earthquakes. The main slip was on the shallowest subfaults in 2011 (Satake et al. 2013b), while it was on the deeper subfaults in 1896

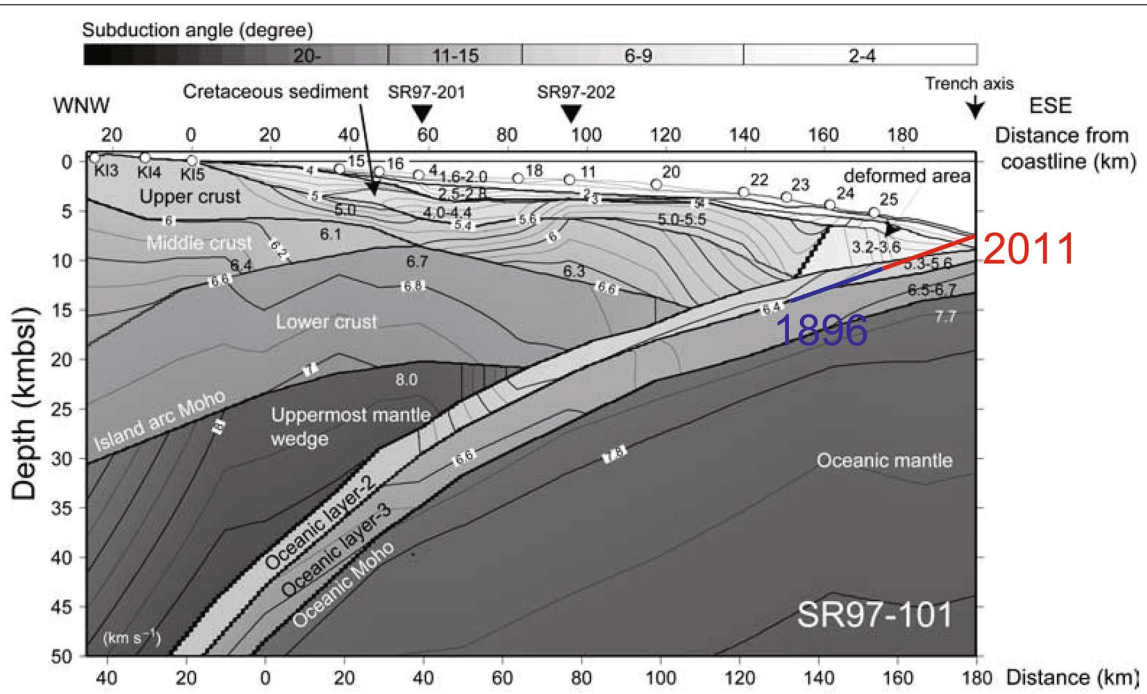

Fig. 6 Velocity structure profile touched in Takahashi et al. (2004). Both 1896 and 2011 slips were on the shallowest part of the subduction zone near trench axis, below low velocity prism

2011 earthquake was not a 'tsunami earthquake.' As indicated in Fig. 1a, the ground shaking was felt in most part of Japan in 2011. However, a careful inspection of Fig. 1a shows that the strong ground shaking was recorded to the south of the epicenter, where large (> 10 m) slip occurred at deeper (> 7 km) subfaults. While the 2011 earthquake has a feature of 'tsunami earthquake' in the northern part of the source, deeper slip in the southern part of the source caused strong ground shaking, hence the 2011 was not a 'tsunami earthquake.'

The delayed rupture along the northern Japan Trench during the 2011 Tohoku earthquake was estimated by tsunami data (Satake et al. 2013a; Tappin et al. 2014), but not recorded on other types (seismographs or high-rate GPS) of data. It was thus attributed as submarine landslide by Tappin et al. (2014). However, comparative multibeam surveys before and after the 2011 Tohoku earthquake in the northern Japan Trench did not detect large bathymetry change indicating large submarine landslide (Fujiwara et al. 2017). The current study clarifies that the 2011 tsunami source was on shallower fault further from the coast than the 1896 Sanriku 'tsunami earthquake' which caused weak ground shaking. Therefore, it is possible that the fault motion was too slow and weak to be detected on seismic or high-rate GPS data.

Conclusions

The 1896 Sanriku 'tsunami earthquake' occurred along Japan Trench north of the 2011 Tohoku earthquake. While the tsunami heights on the northern and central Sanriku coasts were similar for the two tsunamis, the tsunami heights on the southern Sanriku coast and the tsunami waveforms at regional distances were smaller for the 1896 earthquake. To model the 1896 tsunami source, we started from the northern subfaults of the 2011 Tohoku earthquake model, and modified them to obtain the final fault model. The final model is 200 km long, 50 km wide, with the average slip of 8 m, but large (20 m) slips on deeper subfaults. This is contrary to the 2011 Tohoku earthquake model, which had large slips at shallowest subfaults. Thus the slip distributions on shallow parts of plate interface were different for the 1896 Sanriku and 2011 Tohoku earthquakes.

Additional files

Additional file 1: Table S1. Tsunami heights on the Sanriku coast measured by Iki (1897) and computed from six models: 2011 (L 200 km), 2011 (L 150 km), 1896 inversion, 1896 final, uniform slip at 3.5–7 km depth and uniform slip at 0–3.5 km depth.

Additional file 2: Table S2. Tsunami heights on the Sanriku coast measured by Matsuo (1933) and computed from six models: 2011 (L 200 km), 2011 (L 150 km), 1896 inversion, 1896 final, uniform slip at 3.5–7 km depth and uniform slip at 0–3.5 km depth.

Authors' contributions

KS made overall design of the study and drafted the manuscript. YF made tsunami simulation and inversion using the coarse grid. SY made detailed computations on the Sanriku coast with the fine grid for various fault models. All the authors discussed on the manuscript. All authors read and approved the final manuscript.

Author details

[1] Earthquake Research Institute, The University of Tokyo, 1-1-1 Yayoi, Bunkyo-ku, Tokyo 113-0032, Japan. [2] International Institute of Seismology and Earthquake Engineering, Building Research Institute, 1 Tachihara, Tsukuba, Ibaraki 305-0802, Japan. [3] Seamus Ltd, 2235 Kizaki, Kita-ku, Niigata 950-3304, Japan.

Acknowledgements

We thank Dr. David Tappin and an anonymous reviewer for their critical comments on the original manuscript, which helped us to improve the paper. This work was partially supported by JSPS KAKENHI Grant Number JP16H01838.

Competing interests

The authors declare that they have no competing interests.

Availability of data and materials

The data used in this study are from published literature.

Ethics approval and consent to participate

Not applicable.

Funding

JSPS KAKENHI Grant Number JP16H01838.

Publisher's Note

Received: 9 September 2017 Accepted: 7 December 2017
Published online: 20 December 2017

References

Abe K (1979) Size of great earthquakes of 1873–1974 inferred from tsunami data. J Geophys Res 84:1561–1568

Abe K (1981) Physical size of tsunamigenic earthquakes of the northwestern Pacific. Phys Earth Planet Inter 27:194–205

Abe K (1994) Instrumental magnitudes of historical earthquakes, 1892–1898. Bull Seismol Soc Am 84:415–425

Aida I (1978) Reliability of a tsunami source model derived from fault parameters. J Phys Earth 26:57–73

Central Meteorological Observatory (1902) On the earthquakes in the year 1896 in annual report. Central Meteorological Observatory of Japan, Tokyo

Fujii Y, Satake K, Sakai S, Shinohara M, Kanazawa T (2011) Tsunami source of the 2011 off the Pacific coast of Tohoku Earthquake. Earth Planets Space 63:815–820. https://doi.org/10.5047/eps.2011.06.010

Fujiwara T, dos Ferreira Santos C, Bachmann AK, Strasser M, Wefer G, Sun T, Kanamatsu T, Kodaira S (2017) Seafloor displacement after the 2011 Tohoku-oki earthquake in the northern Japan Trench examined by repeated bathymetric surveys. Geophys Res Lett. https://doi.org/10.1002/2017gl075839

Honda K, Terada T, Yoshida Y, Isitani D (1908) Secondary undulations of oceanic tides. Pub Earthq Invest Comm 26:1–113

Ide S, Baltay A, Beroza GC (2011) Shallow dynamic overshoot and energetic deep rupture in the 2011 M_w 9.0 Tohoku-Oki earthquake. Science 332:1426–1429. https://doi.org/10.1126/science.1207020

Iinuma T, Hino R, Kido M, Inazu D, Osada Y, Ito Y, Ohzono M, Tsushima H, Suzuki S, Fujimoto H, Miura S (2012) Coseismic slip distribution of the 2011 off the Pacific Coast of Tohoku earthquake (*M* 9.0) refined by means of seafloor geodetic data. J Geophys Res 117:B707409. https://doi.org/10.1029/2012JB009186

Iki T (1897) Field survey report of the 1896 Sanriku tsunami. Rep Imp Earthq Invest Comm 11:5–34 **(in Japanese)**
Imamura A, Moriya M (1939) Mareographic observations of tunamis in Japan during the period from 1894 to 1924. Jpn J Astron Geophys 17:119–140
Kanamori H (1972) Mechanism of tsunami earthquakes. Phys Earth Planet Inter 6:246–259
Lay T, Kanamori H, Ammon CJ, Koper KD, Hutko AR, Ye L, Yue H, Rushing TM (2012) Depth-varying rupture properties of subduction zone megathrust faults. J Geophys Res 117:B04311. https://doi.org/10.1029/2011JB009133
Matsuo H (1933) Report on the survey of the 1933 Sanriku tsunami. Rep Civil Eng Lab 24:83–136 **(in Japanese)**
Nakajima J, Hasegawa A (2006) Anomalous low-velocity zone and linear alignment of seismicity along it in the subducted Pacific slab beneath Kanto, Japan: reactivation of subducted fracture zone? Geophys Res Lett 33:L16309. https://doi.org/10.1029/2006GL026773
Okada Y (1985) Surface deformation due to shear and tensile faults in a half-space. Bull Seismol Soc Am 75:135–1154
Omori F, Hirata K (1899) Earthquake measurement at Miyako. J Sci Coll Imp Univ Tokyo 11:61–195
Polet J, Kanamori H (2000) Shallow subduction zone earthquakes and their tsunamigenic potential. Geophys J Int 142:684–702. https://doi.org/10.1046/j.1365-246x.2000.00205.x
Satake K (1995) Linear and nonlinear computations of the 1992 Nicaragua earthquake tsunami. Pure Appl Geophys 144:455–470
Satake K, Tanioka Y (1999) Sources of tsunami and tsunamigenic earthquakes in subduction zones. Pure Appl Geophys 154:467–483
Satake K, Nishimura Y, Putra PS, Gusman AR, Sunendar H, Fujii Y, Tanioka Y, Latief H, Yulianto E (2013a) Tsunami source of the 2010 Mentawai, Indonesia earthquake inferred from tsunami field survey and waveform modeling. Pure Appl Geophys 170:1567–1582. https://doi.org/10.1007/s00024-012-0536-y
Satake K, Fujii Y, Harada T, Namegaya Y (2013b) Time and space distribution of coseismic slip of the 2011 Tohoku earthquake as inferred from tsunami waveform data. Bull Seismol Soc Am 103:1473–1492. https://doi.org/10.1785/0120120122
Sella GF, Dixon TH, Mao AL (2002) REVEL: a model for recent plate velocities from space geodesy. J Geophys Res 107:11–30. https://doi.org/10.1029/2000jb000033
Shuto N, Imamura F, Koshimura S, Satake K, Matsutomi H (2007) Encyclopedia of tsunamis (Tsunami no Jiten). Asakura Publishing, Tokyo, p 350
Takahashi N, Kodaira S, Tsuru T, Park J-O, Kaneda Y, Suyehiro K, Kinoshita J, Abe S, Nishino M, Hino R (2004) Seismic structure and seismogenesis off Sanriku region, northeastern Japan. Geophys J Int 159:129–145. https://doi.org/10.1111/j.1365-246X.2004.02350.x
Tanioka Y, Satake K (1996a) Tsunami generation by horizontal displacement of ocean bottom. Geophys Res Lett 23:861–864
Tanioka Y, Satake K (1996b) Fault parameters of the 1896 Sanriku tsunami earthquake estimated from tsunami numerical modeling. Geophys Res Lett 23:1522–1549
Tanioka Y, Seno T (2001) Sediment effect on tsunami generation of the 1896 Sanriku tsunami earthquake. Geophys Res Lett 28:3389–3392
Tanioka Y, Ruff L, Satake K (1997) What controls the lateral variation of large earthquake occurrence along the Japan Trench? Isl Arc 6:261–266
Tappin DR, Grilli ST, Harris JC, Geller RJ, Masterlark T, Kirby JT, Shi F, Ma G, Thingbaijam KKS, Mai PM (2014) Did a submarine landslide contribute to the 2011 Tohoku tsunami? Mar Geol 357:344–361. https://doi.org/10.1016/j.margeo.2014.09.043
Tsuji Y, Satake K, Ishibe T, Harada T, Nishiyama A, Kusumoto S (2014) Tsunami heights along the Pacific coast of Northern Honshu recorded from the 2011 Tohoku and previous great earthquakes. Pure Appl Geophys 171:3183–3215. https://doi.org/10.1007/s00024-014-0779-x
Unohana M, Ota T (1988) Disaster records of Meiji Sanriku tsunami by Soshin Yamana. Res Rep Tsunami Disaster Prev Lab Fac Civil Eng Tohoku Univ 5:57–379 **(in Japanese)**
Utsu T (1979) Seismicity of Japan from 1885 through 1925. Bull Earthq Res Inst Univ Tokyo 54:253–308
Utsu T (1994) Aftershock activity of the 1896 Sanriku earthquake. Zisin (J Seis. Soc Japan) 2(47):89–92 **(in Japanese)**